International Journal of Thermophysics, Vol. 16, No. 6, 1995

Photothermal Deflection in a Supercritical Fluid

M. E. Briggs[1,2] and R. W. Gammon[1]

November 17, 1994

Photothermal deflection is among the most sensitive techniques available for the measurement of small, localized heating, such as that from the absorption of a focused laser beam in the bulk or surface of a material. A thin optical probe beam is deflected by the refractive-index gradients arising from the heating, and the size of the deflection provides the measure of the heating. We describe the use of a critical fluid to enhance the sensitivity of the technique by at least 10^3. The diverging coefficient of thermal expansion of a pure fluid near the gas–liquid critical point gives this dramatic enhancement when used as a sensing fluid. With sensitivity calculations and measurements in supercritical xenon, $T_c \approx 16.7°C$, we show that the noise floor of our apparatus when used for surface absorption measurements corresponds to a fractional power absorbed of $P_{\text{absorbed}}/P_{\text{incident}} = 10^{-10}$, while the noise floor for bulk measurements corresponds to an absorption coefficient $\alpha = 10^{-13}\,\text{cm}^{-1}$. We report the first measurements of the surface absorption of superpolished surfaces of sapphire and fused quartz, $P_a/P_i \approx 2 \times 10^{-5}$, and the first measurements of the bulk absorption in xenon, $\alpha \approx 2 \times 10^{-6}\,\text{cm}^{-1}$. We also show how the present work fits into the current status of absorption measurement techniques and describe the effects of the peculiar properties of critical fluids on the execution of photothermal deflection measurements.

KEY WORDS: absorption; critical; photothermal deflection; photothermal method; spectroscopy; supercritical; surface.

1. INTRODUCTION

The most sensitive techniques available for the detection of very sall temperature gradients in transparent materials are optical techniques. A probe beam passing through a heated region is deflected and suffers a phase shift from the refractive-index gradients that arise from thermal expansion.

[1] Institute for Physical Science and Technology, University of Maryland, College Park, Maryland 20742-2431, U.S.A.

[2] To whom correspondence should be addressed.

0195-928X/95/1100-1439$07.50/0

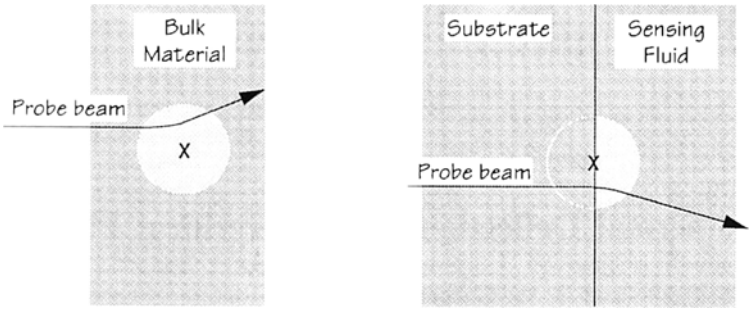

Fig. 1. The optical effects of the thermal expansion around a hot spot at X in the bulk of a transparent material and at the surface of a transparent material. For the surface case, the thermal expansion in the sensing fluid dominates the density effect in the solid substrate.

These effects can be used in experiments on both bulk materials and surfaces, as depicted in Fig. 1. There are many photothermal spectroscopies, where an excitation is created by the absorption of radiation and decays mainly by thermal diffusion. The strength and dynamics of the signal in these techniques provide information about the processes governing the heating—for example, the relaxation of electrons and heat excited in a semiconductor surface by a pulsed pump laser can be monitored from the resulting heat in a fluid above the surface [1], and the presence and concentration of impurities in transparent samples can be deduced from the heat generated by the absorption of a laser beam in the bulk of the sample. The number of applications has grown with the widespread availability of powerful lasers and high-resolution position sensors for optical beams.

This paper describes the enhancement to these techniques through the use of a supercritical fluid as the sensing fluid. The enhancement arises because the signal is created from the thermal expansion of the sensing fluid and the thermal-expansion coefficient of a pure fluid diverges as the state of the fluid approaches the liquid–vapor critical point. At the critical density ρ_c and at a temperature 10 K above the critical point of xenon, $T_c = 16.7°C$, the isobaric thermal-expansion coefficient $\beta_p \equiv (1/\rho)\,\partial\rho/\partial T = 9 \times 10^{-2}\,K^{-1}$, about 100× larger than noncritical fluids. By $T - T_c = 1$ mK, β_p has further increased by 4 decades. By using a sample of supercritical xenon in a photothermal-deflection apparatus, we measure three decades enhancement over the sensitivity reported by other workers with noncritical fluids, making the supercritical method far more sensitive than any other available.

We do not discuss the details of either the calculations of the apparatus here; these are sufficiently important and lengthy to reserve for

a separate publication [2]. Workers in the thermal wave community will need to consider these before assessing the feasibility of working with a supercritical sensing fluid, the difficulties of which we list in Section 4.2. The present paper starts with a brief description of the apparatus. Working equations are presented in Section 3, including new results for surface absorptions and a discussion of the origin of the supercritical enhancement. In Section 4 we present the results of our measurements and calculations, which are done with *no free parameters*, and are summarized in Figs. 3 and 5. We end our paper with a discussion of how the new sensitivity levels fit into the current picture of absorption measurement techniques (Section 5).

2. APPARATUS

We built a conventional photothermal-deflection device, similar to that used by Boccara et al. [3]. Figure 2 shows a schematic of the device making a measurement of the absorption in the bulk of a transparent sample. Two optical beams are used, a broad heating beam and a narrow probe beam. The spatial location where the device measures the absorption is determined by the crossing of the beams; for a surface absorption, the surface is placed adjacent to this crossing. A chopper modulates the heating beam, and a lock-in measures the resulting oscillation in the position of the probe beam that arises from the processes shown in Fig. 1. We calculate the angular deflection from the geometry of the experiment (Section 3).

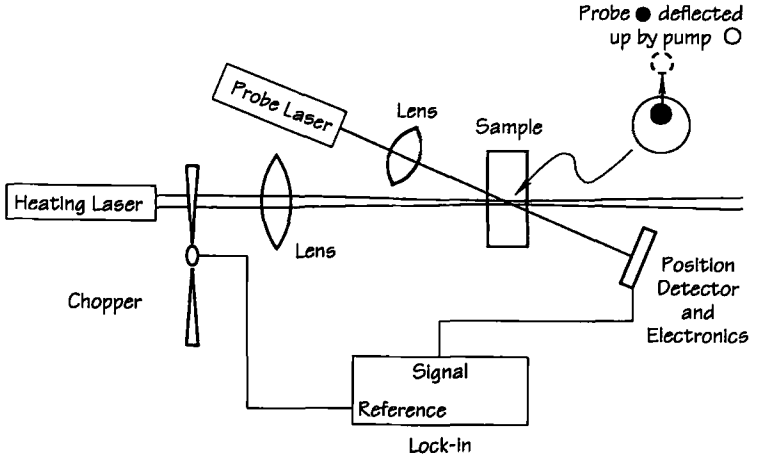

Fig. 2. A schematic of a collinear photothermal deflection apparatus. It is shown making a measurement of the bulk absorption of the heating laser in a transparent sample.

High sensitivity is obtained with the high-resolution position measurement that can be made using the combination of a beam-position detector [4] and lock-in detection. We measure the rms oscillation of the probe-beam position to a resolution of 3 nm (10^{-8} rad), for modulation frequencies above 40 Hz. At frequencies below 1 Hz, analog lock-ins work poorly, so we use a computer to average 10–20 cycles of the signal as captured by a digital volt-meter, for a noise level of about 25 nm (about 10^{-7} rad). The position detector provides the dc position of a beam to a resolution of $\pm 5\,\mu$m, or about 10^{-5} rad in our device, limited by vibrations and by the flow of dust across the beam.

3. CALCULATIONS

Jackson et al. [5] published the general solution and the working equations in several important limiting cases. We will add one important case, the expressions for deflection at a surface absorption when the thermal properties of *both* the substrate and the detection fluid must be retained; the values of the thermal diffusivity and thermal conductivity of the fluid and substrate are comparable in the $3\,\text{mK} \leqslant T - T_c \leqslant 10\,\text{K}$ temperature range spanned by our measurements.

3.1. The Optical and Heat Equations

The equations we derive describe the deflection of a ray of light by the thermal distortion created by a heating beam in an absorptive sample. The problem divides naturally into two parts, the propagation of the ray and the thermal distortion. Because the deflections are very small (the order of μrad), the ray can be assumed to be perpendicular to the refractive-index gradients at all times. If the ray is traveling in the z direction in a medium with cylindrical symmetry about z, and if the temperature gradients are in the radial direction r, then (see, e.g., Ref. 6), the deflection angle will be

$$\theta = \frac{1}{n}\frac{\partial n}{\partial \rho}\frac{\partial \rho}{\partial T}\int_0^\infty \frac{\partial T}{\partial r}\,dz \tag{1}$$

where ρ is the density, the direct dependence of the refractive index n on temperature is negligible, and we have excluded any sources of density variation besides thermal expansion.

To obtain the temperature gradient, we solve the heat equation with the appropriate source term and boundary conditions. The correct description of heat flow in compressible fluids has been shown by Onuki et al. [7] and Boukari et al. [8] to require the addition of a term to the heat

equation describing the adiabatic transfer of heat. However, one of the interesting things about the photothermal technique is that it senses only the temperature gradients that drive this effect, not the uniform temperature rise that results. Therefore, the correct heat equation is the usual

$$\frac{\partial T}{\partial t} = D\,\nabla^2 T + \frac{1}{\rho c_p}\,\dot{Q} \tag{2}$$

where D is the thermal diffusivity of the material, ρ is the density, c_p is the heat capacity per unit mass, and $\dot{Q}$ is the source, in our case the absorption of a heating beam.

Take the heating beam to be propagating in the z direction with power P. We assume a Gaussian intensity profile with a waist radius w_0, that is chopped (100% modulation) at frequency $f = \omega/2\pi$ in a square wave. This heating beam can be described in space and time by

$$I(r, t) = \frac{2P}{\pi w_0^2}\, e^{-2r^2/w_0^2} \left\{ \frac{1}{2} \left(1 + \frac{4}{\pi} \left(\cos \omega t + \frac{1}{3} \cos 3\omega t + \cdots \right) \right) \right\} \tag{3}$$

The distance from the axis of the heating beam is r, and the term in the brackets is the Fourier series of a unit square wave. Attenuation of the beam can be neglected for work on the transparent materials considered here, so that the deposition of heat in the sample is $\dot{Q} = I(r, t)\,\alpha$ (power/volume), where α is the absorption coefficient (cm^{-1}) of the material. For absorption at a surface, α is replaced by the absorptance A, the fractional absorption at the surface $A \equiv P_{\text{absorbed}}/P_{\text{incident}}$, and the source term is $I(r, t)\,A$ (power/area). Finally, the boundary conditions are those of an infinite homogeneous absorptive medium for the case of a bulk absorption or two semiinfinite nonabsorbing media with absorption at the interface, for the case of a surface absorption.

3.2. The Working Equations

The solutions to Eqs. (1) and (2) can be found in several ways, with the result being integral solutions that can be solved analytically only in special cases of high or low frequencies. Our solution is based on the work of Fournier and Boccara [9]. For modulation frequencies less than a rolloff frequency f_r,

$$f_r \equiv 4D/(\pi w_0^2) \tag{4}$$

the low-frequency form applies, and for frequencies greater than f_r, the high-frequency form applies. f_r is a parameter in the integral solutions that

characterizes the relative importance of the conductive and diffusive terms; it is related to the time for heat to diffuse one heating-beam diameter. We obtain the working equations from these limits by substituting the resulting expressions for the temperature gradients into the deflection equation, Eq. (1).

For absorption in the bulk, the rms deflection-angle amplitude for a probe at a distance r from the axis of the heating beam at low modulation frequencies is

$$\theta_{\text{rms}} = \frac{\beta_p}{\Lambda} \frac{1}{n} \frac{\partial n}{\partial \rho} \frac{\alpha l P}{\sqrt{2}\,\pi^2 w_0} \left[\frac{1 - e^{-2r^2/w_0^2}}{r/w_0} \right] \tag{5}$$

and the signal is in phase with the heating beam, while the rms deflection-angle amplitude at high modulation frequencies is

$$\theta_{\text{rms}} = \frac{\beta_p}{\omega \rho c_p} \frac{1}{n} \frac{\partial n}{\partial \rho} \frac{16 \alpha l P}{\sqrt{2}\,\pi^2 w_0^3} \left[\frac{r}{w_0} e^{-2r^2/w_0^2} \right] \tag{6}$$

and the signal lags the heating beam by 90°. Parameters in the above are the thermal diffusivity $D \equiv \Lambda/\rho c_p$, the thermal conductivity Λ, the density ρ, the isobaric specific heat c_p, the isobaric thermal-expansion coefficient β_p, the refractive index n, the absorption coefficient α, the interaction length (overlap) between the heating and the probe beams l, and the power in the heating beam P, and w_0 is the waist radius of the heating beam as defined in Eq. (3).

For absorption at a surface, we have generalized the published results of Commandré and Pelletier [10] for absorption at the surface of a substrate to include the thermal properties of both the substrate and fluid. If A is again the absorptance of the surface ($\equiv P_a/P_i$), the deflection at low frequencies is

$$\theta_{\text{rms}} = \frac{\beta_p}{\Lambda_g + \Lambda_f} \frac{1}{n} \frac{\partial n}{\partial \rho} \frac{PA}{\sqrt{2}\,\pi^2 w_0} \left[\frac{1 - e^{-2r^2/w_0^2}}{r/w_0} \right] \tag{7}$$

and at high frequencies,

$$\theta_{\text{rms}} = \frac{\beta_p}{\omega (\rho c_p)_f} \frac{1}{1 + (\Lambda_g l_f / \Lambda_f l_g)} \frac{1}{n} \frac{\partial n}{\partial \rho} \frac{16 PA}{\sqrt{2}\,\pi^2 w_0^3} \left[\frac{r}{w_0} e^{-2r^2/w_0^2} \right] \tag{8}$$

Again, the signal is in phase with the heating beam at low frequencies and lags by 90° at high frequencies. The only new parameters here are the thermal-diffusion lengths in the fluid and glass, l_f and l_g, which characterize

the decay of the temperature field away from the planar heat source at the interface, $l_{f,g} \equiv \sqrt{2D_{f,g}/\omega}$. The rolloff frequency is $f_r = \sqrt{2D_f/\omega}$ because the slow diffusion in the fluid dominates the relaxation.

3.3. The Supercritical Enhancement

All three thermodynamic properties in the above results—β_p, Λ, and c_p—diverge as a fluid nears the critical point! The signal depends on the *relative* rates of divergence of the coefficient of thermal expansion to the thermal conductivity, β_p/Λ, in the low-frequency case [Eqs. (5) and (7)], or to the specific heat, β_p/c_p, at high frequencies [Eqs. (6) and (8)]. At the critical density, β_p and c_p both diverge with the same exponent, $\sim(T-T_c)^{-1.24}$, but $\Lambda \sim (T-T_c)^{-0.58}$. We have our most important result: the low-frequency signal strength diverges as $T \to T_c$, as $\beta_p/\Lambda \sim (T-T_c)^{-0.66}$! Note, further, that as the sample approaches the critical temperature, the rolloff frequency will go to zero, because $D \to 0$, so that the $1/\omega$ high-frequency behavior will extend to lower frequencies. Response at any particular frequency in the high-frequency regime will saturate as $T \to T_c$, reflecting the fact that the thermal expansion coefficient and specific heat diverge with the same exponent (for discussions of critical exponents and behavior, see, e.g., Refs. 11 and 12). Note that all the parameters in the above expressions are known or measurable, allowing a direct comparison to our data without free parameters.

4. MEASUREMENTS

Our discovery of the size of the above optical effects in compressible fluids came by accident in trying to understand speckle motion around a 1-mW laser after it passed through a critical-xenon sample: the speckle seemed to flow up around the beam, suggesting convection around a heat source. After we realized the implications for photothermal techniques, and that these had gone unnoticed, we set out to characterize the response of our critical sample in a photothermal device as a function of proximity to T_c.

4.1. Calibration

Our first step in characterizing the supercritical response was to calibrate the device we built and use it to measure the absorptance of the antireflection coatings used in the xenon cell. To this end, we immersed a calibrated absorber into a cuvette containing carbon tetrachloride (CCl_4)

and made a study of signal strength vs frequency. The calibrated absorber was a piece of a metal-film neutral density filter with an absorption of 11%, determined by measuring the reflected, transmitted, and incident power of a beam passing through the filter. The signals from this piece in the photothermal apparatus provide the conversion between signal strength and surface absorptance A. Two spare cell windows from the batch from which our xenon cell was constructed were then inserted in place of the calibrator piece, and the absorptances of the coatings were noted. The absorptances of the window surfaces were the same, so that we could assign with confidence an absorptance to the surfaces in the xenon cell, $A = 1.4 \times 10^{-4} \pm 20\%$ for each surface. The error here is the reproducibility of the measurements, coming from the variation in the absorptance over a

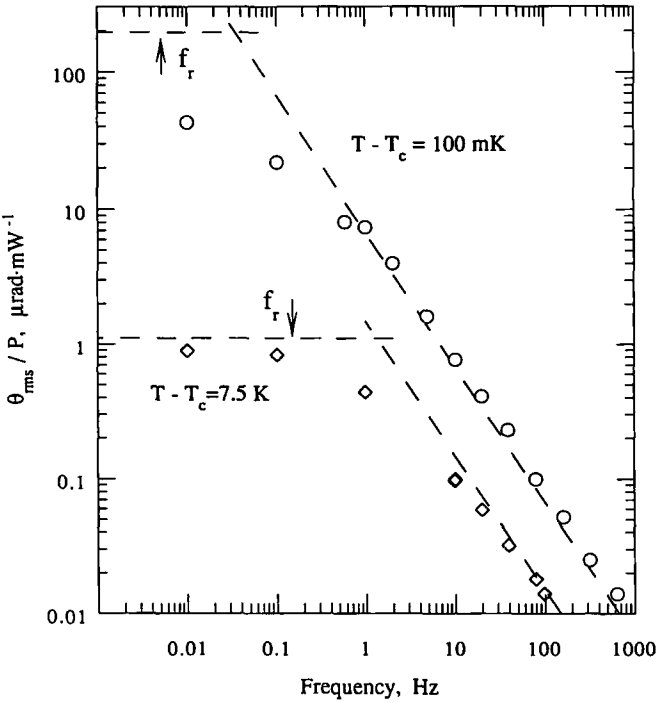

Fig. 3. Signal strength vs frequency at $T - T_c = 7.5$ and 0.1 K at the 200-μm waist radius focus for a xenon sample at the critical density. f_r is the rolloff frequency described in Section 3.1. The symbols are data, with uncertainty approximately the size of the symbol, and the dashed lines are calculated from the limiting forms of the working equations, Eqs. (5)–(8), with no adjustable parameters.

particular window surface, and the error in positioning the surface, the probe, and the heating beam waists at the same place.

4.2. The Supercritical Measurements

Knowing the absorptance of the antireflection-coated window surfaces of our xenon cell, we inserted the cell, enclosed in a thermostat, into the apparatus. A detailed presentation will be made in Ref. 2; the essential points to mention here are that critical-point optical cells must seal against high pressure, 58 atm for xenon, and that the temperature must be controlled to ± 1 mK for the full enhancement we report. An improvement of 200× is still available just from a bare cell sitting in a room controlled to a few degrees, as the critical temperature $T_c = 16.7°C$ happens to fall sufficiently below the room temperature to be out of the highly unstable region of the fluid, while still sufficiently close that the thermal expansion coefficient is anomolously large. The stability and linearity of the signal are good, given that the intensity of the heating beam is kept sufficiently low, as noted in the discussion of Fig. 4 below.

We measured the deflection amplitude and phase as a function of frequency at temperatures from $T - T_c = 10$ K to $T - T_c = 3$ mK; the critical temperature in the sample was known to within 1 mK from transmission and scattering measurements in a different apparatus. This set of measurements was made with a heating-beam waist radius of 200 μm,

Table I. Optical and Thermophysical Properties for Fused Silica, CCl_4, and Xenon[a]

Property	Units	Symbol	CCl_4[b]	Xenon[c]	Fused silica[d]
Density	$kg \cdot m^{-3}$	ρ	1.594×10^3	1.110×10^3	2.20×10^3
Refractive index		n	1.4579	1.13665	1.457
Isobaric specific heat	$J \cdot kg^{-1} \cdot K^{-1}$	c_p	8.41×10^2	3.68×10^3	7.41×10^2
Thermal conductivity	$W \cdot m^{-1} \cdot K^{-1}$	Λ	0.105	0.0387	1.38
Thermal diffusivity	$m^2 \cdot s^{-1}$	$D \equiv \Lambda/(\rho c_p)$	7.84×10^{-6}	9.49×10^{-9}	8.5×10^{-7}
Specific heat ratio		$\gamma \equiv c_p/c_v$	1.47	1.72×10^1	
Isobaric thermal-expansion coefficient	K^{-1}	β_p	1.24×10^{-3}	9.10×10^{-2}	
Isothermal compressibility	$m^2 \cdot N^{-1}$	κ_T	1.08×10^{-9}	6.45×10^{-7}	

[a] Data for fused silica and CCl_4 are for a temperature of 20°C and a pressure of 1 atm. Data for xenon are included for comparison, for a temperature of 27°C ($T - T_c = 10$ K) and a density $\rho = \rho_c = 1.11\ g \cdot cm^{-3}$. The critical pressure for xenon (i.e., P at ρ_c, T_c) is $P_c = 58.4$ atm. Critical parameters come from Sengers and Levelt Sengers [15].

[b] ρ, n at 656 nm; Λ and β_p are from Ref. 17; and c_p is from Ref. 18.

[c] $\rho = \rho_c$, $n = n(\rho_c)$ at 632.8 nm. ρ_c and n are from Moldover et al. [11], and the rest are from the calculations described in Section 3.

[d] ρ, n at 644 nm; Λ is from Ref. 17; and c_p is from Ref. 19.

giving a rolloff frequency [Eq. (4)] between $f_r = 0.12$ cycles/sec at $T - T_c = 10°C$ and $f_r = 4 \times 10^{-4}$ cycles/sec at $T - T_c = 3$ mK. With these low rolloff frequencies, none of the data closer than $T - T_c = 1$ K was in the low-frequency limit.

Figure 3 shows two temperatures from this set, plotted together with the calculation described in Section 3. There are no adjustable parameters in this calculation. The phase of the signal is not shown, but followed the expected limiting behavior, in phase with the heating beam at low frequencies and lagging by 90° at high frequencies. We list the materials parameters in Table I, except for the temperature-dependent xenon parameters, which are calculated using the cubic model (see Ref. 11); the dominant errors are from the measurement and location of the beam waists

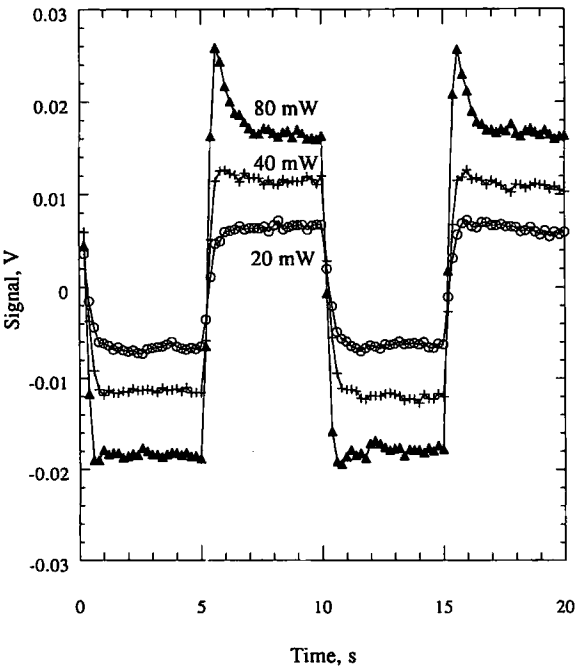

Fig. 4. Deflection vs time data for 0.1-Hz modulation frequency at focus 200 μm, and $T - T_c = 3$ mK, with heating powers of 20, 40, and 80 mW. Note that as the power of the heating beam is increased, the shape of the photothermal response changes from the expected square wave to a cutoff response assumed to arise from convection. The probe in this run is located above the heating beam, and a positive-going signal corresponds to the shutter opening and to the probe deflecting upward.

and from the 20% uncertainty in the coating-absorptance calibration. We made knife-edge measurements of the waists with an accuracy of a few micrometers, so that the accuracy of the calculation for the first run is limited by the 20% accuracy of the absorptance calibration. This is the size of the symbols in the figure.

In an effort to measure in the low-frequency limit, with the temperature still at $T - T_c = 3$ mK, we tightened the focus to raise the rolloff frequency. First at 150 μm, and then at 60 μm, we found that we had to reduce the heating-beam power severely in order to avoid seeing a nonlinear power dependence, and as a result we could not reach the dc response. The nonlinear power dependence was likely to have been a sign of convection; Fig. 4 shows a qualitative change in the waveform consistent with this interpretation. Gupta [13] has developed a formalism that successfully describes the photothermal-deflection response in the presence of

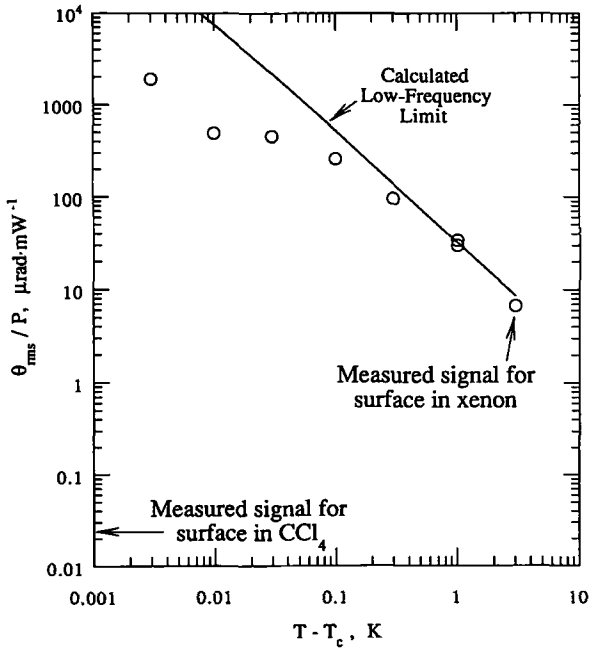

Fig. 5. Our lowest-frequency measurements at our tightest focus (60 μm) reach the low-frequency limited response only for $T - T_c > 0.1$ K. The enhancement is still tremendous: shown for comparison is the response measured in CCl_4. The noise floor for low-frequency measurements is about 0.1 μrad, with typical data taken at a power level chosen to give a signal of 1-μrad rms deflection.

a steady fluid flow; a study of signal strength and phase as a function of power could be compared with these equations to extract the flow velocity. The onset of convection and steady-state flow has not been calculated from first principles for these types of experiments. We mapped the low-frequency response vs T_c at the 60-μm focus, the results of which are collected in Fig. 5. The increasing distance between the data and the calculation as $T \rightarrow T_c$ is consistent with a decreasing rolloff frequency, moving the 0.01 Hz at which the measurements of Fig. 5 were made into the high-frequency characteristic fluid response.

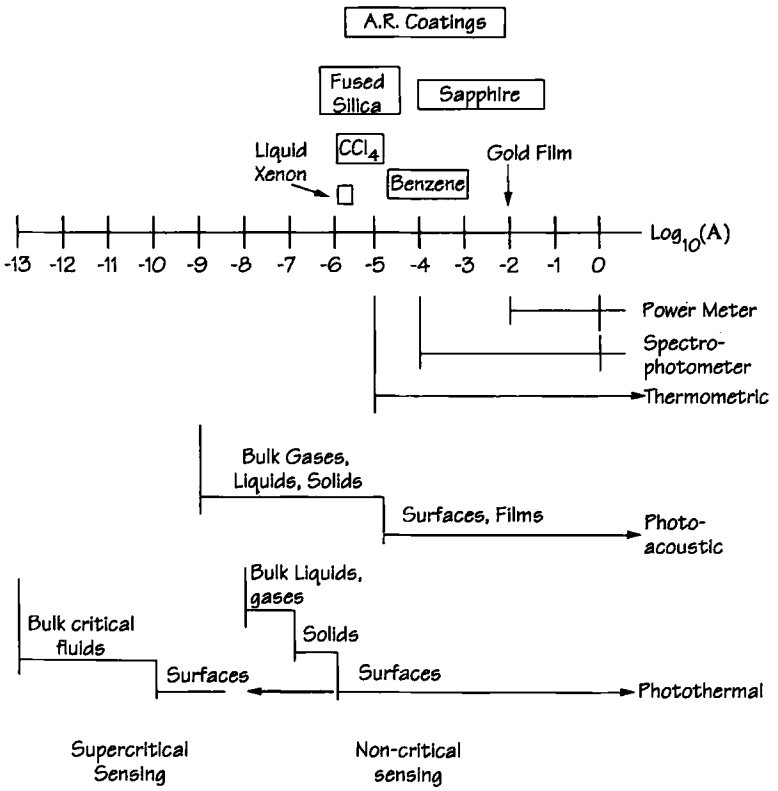

Fig. 6. A logarithmic guide to absorption measurements, giving the minimum detectable fractional absorption, $A \equiv P_{\text{absorbed}}/P_{\text{incident}}$, for various techniques, under a 1-W cw illumination. For bulk absorptions, the length l is taken to be 1 cm, where $A = \alpha l$. The thermometric, photoacoustic, and photothermal techniques can be used with opaque materials.

4.3. The Measured Supercritical Enhancements

In Fig. 5 we have shown for comparison the response we measured in CCl_4 instead of xenon. The CCl_4 data are the measurements used in the calibration of the absorptance of the xenon cell windows (Section 4.1). At room temperature, $T - T_c \approx 10$ K, the xenon response is 75× higher than that of the ordinary fluid. When the sample is brought to $T - T_c = 3$ mK, this ratio has grown to 10^5×, in our low-frequency data. Note that the enhancement listed in the abstract and in Fig. 6 is a conservative value obtained by comparing the noise level of our supercritical xenon work with the published noise levels for other workers' apparatuses.

4.4. New Measurements

In addition to having the world's most sensitive absorption measurement device, we found ourselves in the position of having some of the world's most transparent materials to investigate. A specialty optics company [14] was supplying us with "superpolished" optical windows made of fused silica or sapphire, with and without low-absorbing antireflection coatings, for our critical-fluid space experiment. We were using these to construct xenon critical-point cells under excruciating cleanliness standards in order to ensure a stable critical cell. The polish on the optical surfaces came with characterizations that showed a <10-Å rms surface roughness, and the absorptance of the coating material had been characterized in high-reflection coatings to have a total loss of less than 10^{-6}. We were quite surprised under these conditions to find that the *bare* optical surfaces —both fused silica and sapphire—absorbed 2×10^{-5} of the incident light and that the coated surfaces absorbed double the level of the uncoated surfaces. As a simple model yields a contribution from bulk absorption several decades too low to account for this level [2], the source of this absorptance is not known but will need to be understood before optics can be produced with higher transmission.

Xenon is also very transparent. By translating the cell so that the surfaces were away from the intersection of the probe and heating-beams, we were able to measure the bulk absorption coefficient of the xenon. Using the formalism of Section 3, we found that all of the many xenon cells we were producing had bulk absorptions that were stable at about $2 \times 10^{-6}\,\mathrm{cm}^{-1}$. This removes the xenon as a candidate for the above absorption levels, as the intersection length of the heating and probe beams is about 1 mm, for a contribution of 2×10^{-7}. This also places xenon

among the lowest-absorbing liquids reported; the only other liquid with an absorption coefficient at this level is CCl_4, at $2 \times 10^{-6}\,cm^{-1}$, reported by Jackson et al. [5].

5. CONCLUSIONS

Our results are put in context with other absorption techniques in Fig. 6: instrumental resolution is described by the minimum absorption that could be detected, i.e., the absorption that corresponds to the noise level. Until our work, the limit of sensitivity had not changed much since the work of Boccara et al. [3] and Jackson et al. [5], who achieved noise levels for bulk-absorption measurements corresponding to an absorption coefficient $\alpha = 10^{-8}\,cm^{-1}$, where the fractional absorption in a length z of material is $P_a/P_i = 1 - e^{-\alpha z}$. These workers achieve a noise level for measurements of absorption by a surface of $A \approx 10^{-7}$. The noise level of our bulk-absorption measurements with supercritical xenon corresponds to an absorption coefficient $\alpha \approx 10^{-13}\,cm^{-1}$ for radiation absorbed in the bulk of the sample and $A \approx 10^{-10}$ for radiation absorbed at the surface. The corresponding temperature oscillations are $40\,\mu K_{rms}$ on the axis of the heating beam in the bulk and $13\,nK_{rms}$ on surfaces. That this dramatic increase to the sensitivity could have been overlooked is likely because the divergence in β_p is not widely appreciated outside the small number of groups interested in the liquid–vapor critical point, and constructing the high-pressure cells for pure-fluid critical points requires special efforts.

It is clear that the sensitivity of photothermal measurements is increased so much by the use of a critical fluid that the limits lie in the creativity of the experimenter in devising interesting questions at these low levels, and understanding and circumventing the background absorptions. Already from our work we have an unexpectedly high absorption at bare, superpolished optical surfaces. As an increase in the sensitivity has been called for recently in an overview of the field [16], we hope that our work can provide a means for new results in other areas.

ACKNOWLEDGMENT

This work was supported by the National Aeronautics and Space Administration, Contract No. NAS3-25370.

REFERENCES

1. For a comprehensive list of photothermal applications, see *Photoacoustic and Photothermal Phenomena II*, J. C. Murphy, J. W. Maclachlan Spicer, L. C. Aamodt, and B. S. H. Royce, eds. (Springer-Verlag, New York, 1991).

2. M. E. Briggs and R. W. Gammon, submitted for publication.
3. A. C. Boccara, D. Fournier, W. Jackson, and N. M. Amer, *Opt. Lett.* **5**:377 (1980).
4. United Detector Technologies (UDT) Corporation 1223 Detector head and 431 analog processing electronics, with a 4-kHz bandwidth.
5. W. B. Jackson, N. M. Amer, A. C. Boccara, and D. Fournier, *Appl. Opt.* **20**:1333 (1981).
6. M. V. Klein, *Optics* (Wiley, New York, 1970).
7. A. Onuki, H. Hao, and R. A. Ferrell, *Phys. Rev. A* **41**:2256 (1990).
8. H. Boukari, J. N. Shaumeyer, M. E. Briggs, and R. W. Gammon, *Phys. Rev. A* **41**:2260 (1990).
9. D. Fournier and A. C. Boccara, in *Photothermal Investigations of Solids and Fluids*, J. A. Sell, ed. (Academic Press, San Diego, CA, 1989).
10. M. Commandré and E. Pelletier, *Appl. Opt.* **29**:4276 (1990).
11. M. R. Moldover, J. V. Sengers, R. W. Gammon, and R. J. Hocken, *Rev. Mod. Phys.* **51**:79 (1979).
12. H. E. Stanley, *Introduction to Phase Transitions and Critical Phenomena* (Oxford, New York, 1971).
13. R. Gupta, in *Principles and Perspectives of Photothermal and Photoacoustic Penomena*, A. Mandelis, ed. (Elsevier, New York, 1992).
14. PMS Corporation, Boulder, CO, U.S.A.
15. J. V. Sengers and J. M. H. Levelt Sengers, *Annu. Rev. Phys. Chem.* **37**:189 (1986).
16. A. C. Boccara and D. Fournier, in *Principles and Perspectives of Photothermal and Photoacoustic Phenomena*, A. Mandelis, ed. (Elsevier, New York, 1992).
17. D. E. Gray (ed.), *AIP Handbook of Physics*, 3rd ed. (McGraw–Hill, New York, 1972).
18. R. C. Weast (ed.), *CRC Handbook of Chemistry and Physics*, 60th ed. (CRC Press, Boca Raton, FL, 1980).
19. W. L. Wolf, in *Handbook of Optics*, W. G. Driscoll and W. Vaugham, eds. (McGraw–Hill, New York, 1978).